Offshore Anchor Penetration in Sands: Granular Simulations

Nan Zhang[1], S.M.ASCE and T. Matthew Evans[2], A.M.ASCE

[1] Research Assistant, School of Civil and Construction Engineering, Oregon State University, Corvallis, OR USA
[2] Associate Professor, School of Civil and Construction Engineering, Oregon State University, Corvallis, OR USA, matt.evans@oregonstate.edu

ABSTRACT:

Torpedo anchors are a viable approach for mooring marine hydrokinetic (MHK) energy devices to the seafloor. These anchors will serve to maintain station and to provide the reaction force for the MHK device. The ability of the anchor to perform these duties is a strong function of its penetration depth during installation. This is a large-strain problem not amenable to typical continuum numerical approaches. In the current work, we propose that the discrete element method (DEM) is a more appropriate tool to investigate the shallow penetration of torpedo anchors in sands. The effects of anchor mass, impact velocity, and anchor geometry are considered in the DEM simulations. The relative maximum penetration depths under these factors are quantified and presented in the paper. Comparisons are also made between DEM simulations and the empirical equation developed by Young (1967). Granular material response at the microscale during penetration are used to provide insight into system response.

INTRODUCTION

Offshore dynamically penetrated anchors (DPA), also called "torpedo" anchors or "rocket" anchors, are used for mooring deep water offshore facilities. They are constructed by a cone-tipped cylindrical steel pipe sections filled with concrete or scrap chain and have a pad eye at the top. DPA are penetrated into the seabed by the kinetic energy acquired during the free fall through the water. A mooring line is typically connected to the top of the anchor. The design of DPAs includes the estimation of embedment depth and holding capacities for both long-term and short term. Existing design methods are based on results from both experimental tests and numerical simulations. Physical experiments, including full-scale *in-situ* testing and small-scale centrifuge models, have been performed by many researchers (e.g., True 1976; Freeman et al. 1988; Lieng et al. 1999, 2000; O'Loughlin et al. 2004; Ehlers et al. 2004; Audibert et al. 2006; Shahin and Jaksa 2006; Richardson 2008; O'Loughlin et al. 2009; Raie and Tassoulas 2009; Richardson 2008; Lieng et al. 2010; O'Loughlin et al. 2013; Kim et al. 2014; Hossain et al. 2015). Most of these tests were performed in cohesive soils. The influence of impact velocity on embedment depth is the primary performance metric considered in these studies. The influence of anchor shape and anchor weight on penetration depth are often considered.

Relatively fewer experimental tests have been performed on anchor penetration in sandy soils. Only one instance was found in the literature of field tests on seafloor with sandy soils and cohesive soils on the Brazilian coast (Medeiros et al. 2002). Penetration depths in clay were found to be larger than in sandy soils for the same impact velocities. Instead, projectile penetration tests on granular soils were performed mostly in military areas with very high impact velocities ($\gtrsim$300 m/s) (e.g. Pyrz et al. 1969; Wang 1969; Wang 1971; True 1972; True 1975; Fragaszy et al. 1989; Taylor et al. 1991; Van Vooren et al. 2013). Factors such as projectile nose shape, projectile weight, gravity, and projectile body shape were considered.

Numerical analyses of offshore anchor behavior have been performed by O'Beirne et al. (2015) to compare FEM results with field tests and investigate the soil response of different load inclinations during pullout. Raie and Tassoulas (2009) used computational fluid dynamics (CFD) to simulate soil behaviors under anchor penetration by approximating the soil as a fluid. Numerical analyses on cone penetration tests (similar to the mechanics of DPA) in crushable sands have also been performed (e.g., Ciantia et al. 2016), but analyses to investigate microscale soil performance in the vicinity of anchor penetration have not been reported previously. In the current work, DEM is employed to investigate the microscale response of DPAs in sandy soils.

The discrete element method (DEM) allows for the simulation of soils as a collection of individual particles and is increasingly being applied to a wide array of problems that involve granular materials in contact with geostructures (e.g., Kress and Evans 2010; Evans and Kress 2011). DEM models predict emergent behavior in particulate assemblies based on simulation of independent particle behaviors. DEM has been previously used to study shear bands in sand, including free-field shearing (Jacobsen et al. 2007; Evans and Frost 2010; Zhao and Evans 2011; Frost et al. 2012) and also granular-continuum interface shearing (Dove et al. 2006; Kress and Evans 2010; Evans and Kress 2011; Zhang and Evans 2016). Overall, simulated material response from DEM simulations have been shown to be consistent with results from physical experiments for a variety of loading conditions (Zhao and Evans 2009; Evans and Frost 2010).

Anchor installation is the first step for deploying an offshore anchor system. In the case of DPAs for marine hydrokinetic (MHK) energy generators, anchors serve to keep devices on station and as the reaction force necessary for energy generation. The holding capacity of the anchors must bear the tensile force from ocean waves transmitted by mooring lines. The soil-anchor interface shear force as well as the anchor weight play major roles on the anchor holding capacity. Typically, the deeper the embedment, the higher the holding capacity. Apart from the properties of the seabed soils, the anchor properties (e.g., anchor weight) are combined to determine the holding capacity and allowable reaction force for a given anchor design. Much of the previous work on DPA has focused on FEM analyses, CFD analyses, and/or limit equilibrium solutions and are only applicable to clay sediments (Lieng et al. 2000; Raie and Tassoulas 2009; O'Loughlin et al. 2013; O'Beirne et al. 2015). However, both of these approaches neglect much of the fundamental physics occurring at the anchor-soil interface or do not consider DPAs embedded in sandy soils. This work uses DEM simulations to evaluate the response of DPA penetration into sandy soils.

DEM SIMULATIONS

Prior installation of dynamically penetrated anchors and projectile penetration tests have focused on factors like the impact velocities, nose and shaft shapes, and anchor/projectile weights and their influences on the penetration depths. The simulations below focus on similar effects on the penetration depths in a small scale and explore the microscale responses during penetration.

The geometry of the DEM model of the DPA installation is shown in Figure 1. The assembly consists of a collection of polydisperse spheres intended to simulate sandy soil specimen and larger particle bonded stick-like clump to simulate a DPA. The dimensions of the granular assembly are defined as functions of median particle size d_{50}. Figure 1 shows one penetration state when the DPA has already penetrated into the granular assembly. Mass scaling (e.g., Belheine et al. 2009; Evans and Valdes 2011) is employed to decrease simulation time; as such, the mean particle diameter is d_{50} = 0.5 m and other model dimensions are scaled accordingly. Specifically, model width (W), length (L), and height (H) can be expressed in terms of d_{50} as W/d_{50} = 40, L/d_{50} = 40, and H/d_{50} = 60, respectively. The diameter of the DPA is $D=0.1L=4d_{50}$. Material and model parameters are shown in Table 1.

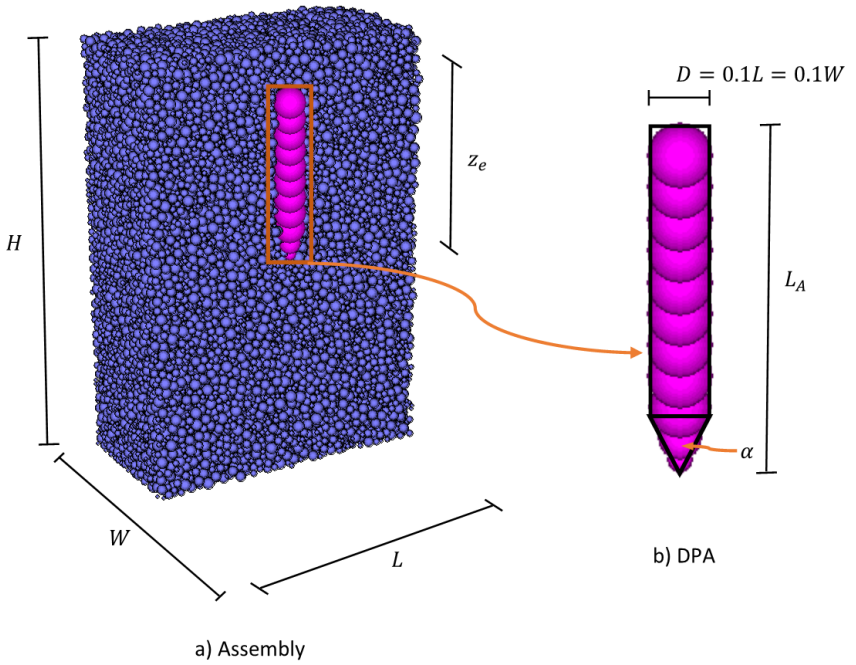

Figure 1. DEM model for DPA penetration.

A scaled gravity value is assigned for the simulation to balance the resultant gravitational force results from mass scaling. The specimen is consolidated in the assigned gravity to equilibrium by cycling the granular assembly to a state where the average unbalanced force in the assembly is less than 1% of the average contact force. This as-consolidated void ratio can be adjusted by varying the particles' and walls' friction coefficients during consolidation, with a higher friction value resulting in a looser specimen. Note that $\mu_c \in [0, \mu]$ where μ_c is the friction coefficient used during consolidation and μ is the actual particle friction coefficient. After consolidation, particle friction can be adjusted to assess the effects of particle friction on pullout resistance. Once the specimen is consolidated and equilibrated, the DPA is generated with anchor tip right above the specimen and released by assigning a negative vertical constant velocity to simulate the impact velocity in practice. Particle motion in the assembly is damped to dissipate excess energy; however, the damping ratio of the clump (i.e., the DPA) is set to be zero to model free fall. Penetration is considered complete when the anchor vertical velocity is very small relative to the impact velocity and close to the mean particle velocity. This velocity is defined as the ending velocity. The

interface shearing force is obtained by measuring the out-of-balance force on the clump. The simulations discussed herein consist of approximately 84,000 particles; one simulation requires roughly five days to complete on an Intel Xeon E5-2660v3 processor on Windows Server 2012.

Table 1. Material and model properties (baseline).

	Parameters	Value
Particles	Maximum diameter, d_{max} [m]	0.75
	Minimum diameter, d_{min} [m]	0.25
	Normal stiffness, k_n [N/m]	1×10^8
	Shear stiffness, k_s [N/m]	8×10^7
	Friction coefficient, μ [ ]	0.31
	Density, ρ_s [kg/m^3]	2650
Model	Height, H [d_{50}]	60
	Width, W [d_{50}]	40
	Length, L[d_{50}]	2×10^7
	Initial porosity [ ]	0.426
DPA	Normal stiffness, k_{sn} [N/m]	1×10^8
	Shear stiffness, k_{ss} [N/m]	8×10^7
	Density, ρ_a [kg/m^3]	1×10^5
	Diameter, D [d_{50}]	4

PARAMETRIC ANALYSIS

Twenty-three simulations were performed to investigate the influence of impact velocity, anchor shape, and anchor weight on penetration depth. The first set focuses on impact velocities, which range from 5 m/s to 25 m/s. The second set focuses on the anchor shapes by changing the number of particles in the anchor shaft from 1 to 8, and the last set focuses on anchor weight by changing the anchor particle density from 0.1 to 1.0ρ_a, where ρ_a is the baseline anchor particle density. Other parameters are kept constant when focusing each of the above three sets. Relative penetration depths for different impact velocities are investigated, where the relative penetration depth is defined as the tip penetration over the anchor length as z_e/L_a (where z_e is anchor tip penetration depth, L_a is anchor length).

In practice, the anchor density is designed to be much larger than the soil density. For the simulations, the anchor particle density is set to be larger than the particle density of granular assembly, see Table 1. At the given volume, the anchor weight can be altered by modifying the anchor particle densities. Anchor shape (specifically, aspect ratio) in the simulations can be described by changing the number of particles in the anchor shaft.

Comparison will be made between DEM models and the empirical equation developed by Young (1967) through dozens of experimental tests. For impact velocities less than 60 m/s:

$$P_m = 0.53SN\frac{W^{\frac{1}{2}}}{A}\ln\left(2\times10^{-5}V_0^2+1\right) \tag{1}$$

where P_m is the penetration depth, W is the weight, A is the area, V_0 is the impact velocity, and S and N are both constants related to the soil properties. According to Young (1967), N is 0.45 and S is equal to 5.

RESULTS AND DISCUSSION

Figure 2 shows the anchor velocities along with penetration depth normalized by the diameter of the anchor under different impact velocities. It is clear that higher impact velocities result in higher velocities at the same normalized penetration depth (z_e/D). The velocity of real soil particles in a static state is zero. However, the velocity of particles in DEM simulations are never identically zero due to numerical vibrations in the system. Thus, the velocity of the anchor penetrated into the granular assembly will not be zero even at the equilibrium state. For the simulations, an ending velocity at which the simulation will be terminated should be specified. The ending velocity for all the simulations reported herein was set as 1 m/s. The maximum penetration depths are the anchor tip penetration depths when the vertical anchor velocity equals the ending velocity. The anchor with the highest velocity has the largest kinetic energy. It will take longer to release its kinetic energy. The penetration depth will be larger as a result.

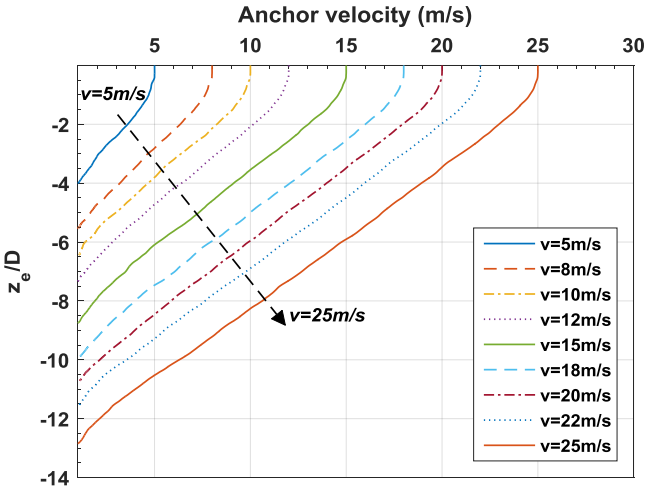

Figure 2. Anchor velocity profile during penetration under different impact velocities

Maximum penetration depths under different impact velocities are shown in Figure 3(a) below. The maximum penetration depths are normalized by the anchor length L_a as the relative penetration depth. Results can be found that the higher the impact velocity, the higher the maximum penetration depth. The negative symbol in Figure 3 means the direction relative to the surface. The maximum tip penetration depths at higher impact velocities (v = 22 m/s and 25 m/s) are more than twice the length of the anchor. However, the value for lower impact velocities are near the length of the anchor.

Another factor that affects penetration is anchor weight. The anchor weight can be calculated from multiplying anchor density by anchor volume. Figure 3(b) shows the maximum relative penetration depth as a function of normalized anchor weight. Normalized anchor weight is defined as the ratio of anchor weight to the anchor weight at baseline. The impact velocity is set as 20 m/s.

Simulation results show that the higher the anchor weight, the larger the maximum relative penetration depth. Maximum penetration depth increases approximately linearly with anchor weight.

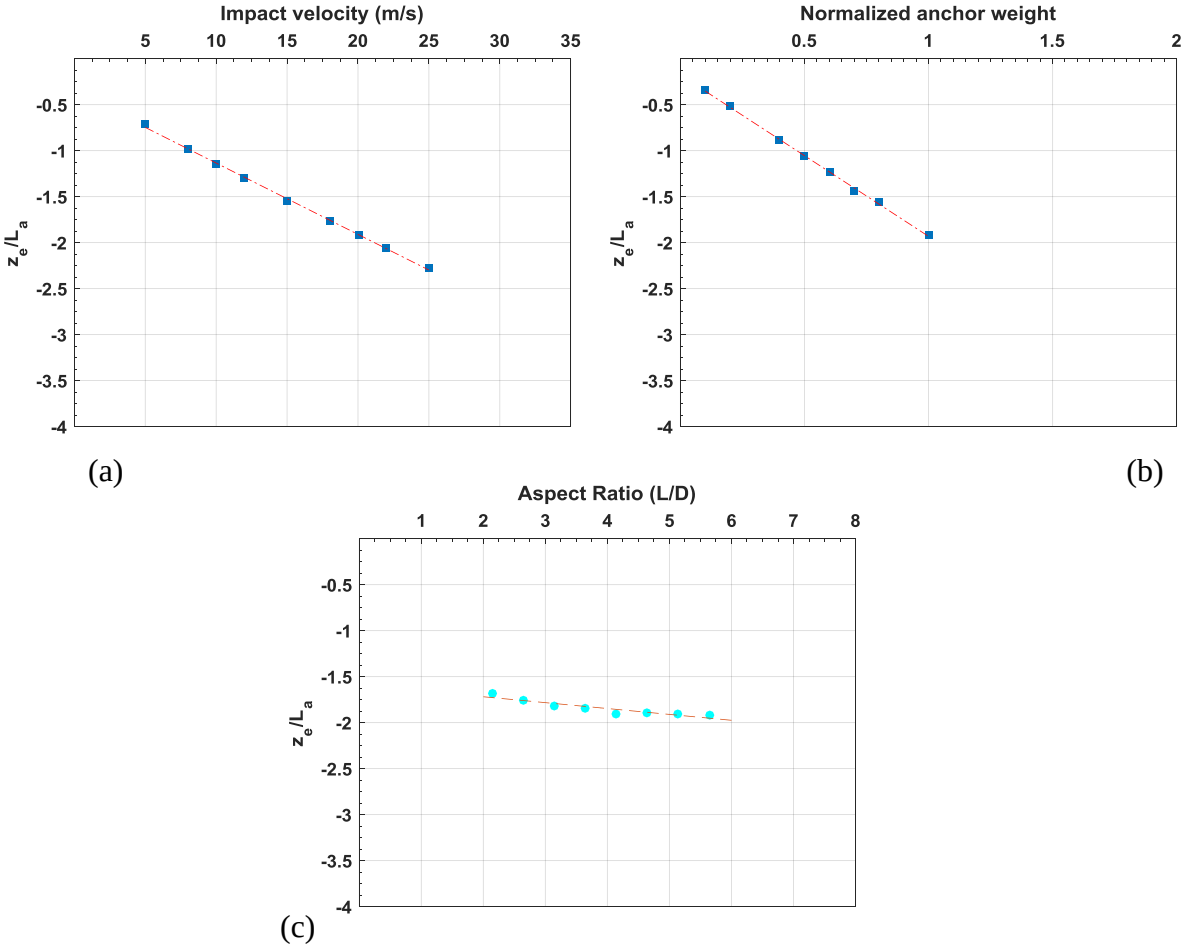

Figure 3. Maximum relative penetration depth under a) different impact velocities, b) under different normalized anchor weights, and c) under different anchor aspect ratios

Anchor shape (aspect ratio) ranges from 2.14 to 5.64 in the simulations. Figure 3(c) shows the maximum relative penetration depth for different anchor aspect ratios. The maximum relative penetration depths vary over a narrow range (i.e. from 0.7 to 2.0). These results support the idea that anchor shape has less significance than anchor impact velocity and anchor weight.

Figure 4 shows one penetration state of the granular assembly. The left figure shows the particle impact responses and the right figure shows the particle velocity vectors at this state. Particles at the surface are disturbed the most. The particles are jumping up to flow away from the assembly and then will return to the assembly under gravity, see the left side of Figure 4. Particles around the anchor tip are also highly disturbed, as shown in the right side of Figure 4.

Figure 5 shows the maximum relative penetration depth comparisons between DEM simulations and the results obtained from Equation 1. Comparing to Young (1967), DEM simulations give a linear relationship while the empirical equation gives a nonlinear one. The penetration depths are aggressive and conservative at lower and higher impact velocities, respectively, compared to the

Young (1967) empirical equation. Figure 6 shows the contact numbers during penetration under different impact velocities, different aspect ratios and different density, respectively. Contact numbers are normalized by the initial contact numbers (the value before penetration). The maximum percentage of contact number loss under all the three conditions are around 23%. Penetrations result in the contact loses with a large percentage even at the end of penetration, ~15%.

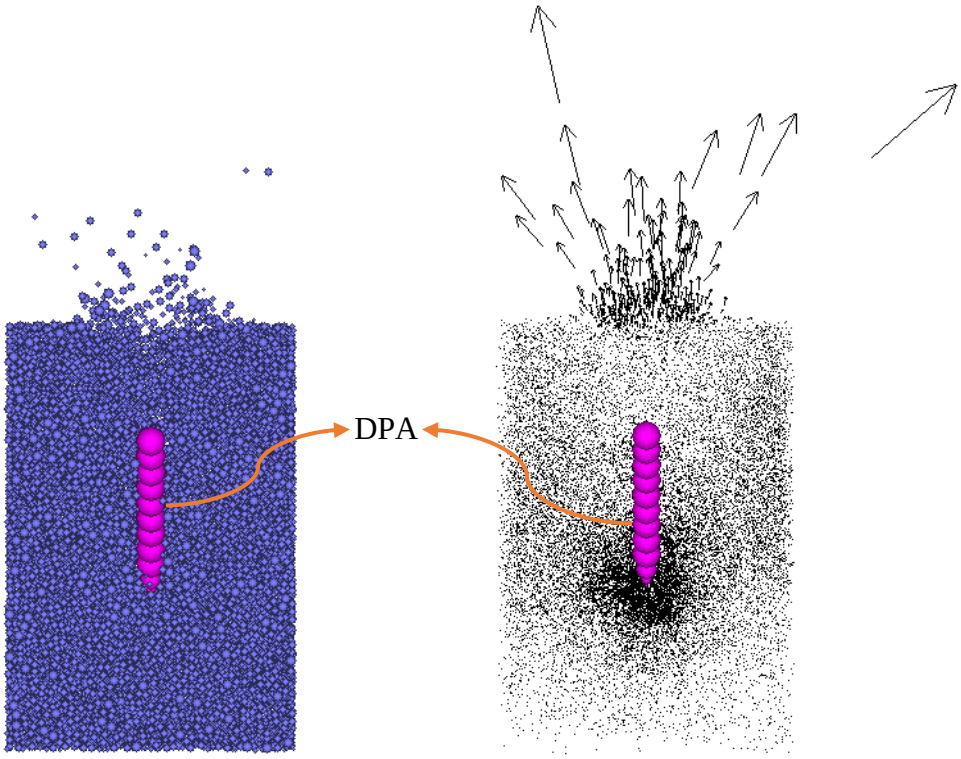

Figure 4. Velocity vectors of particles during penetration

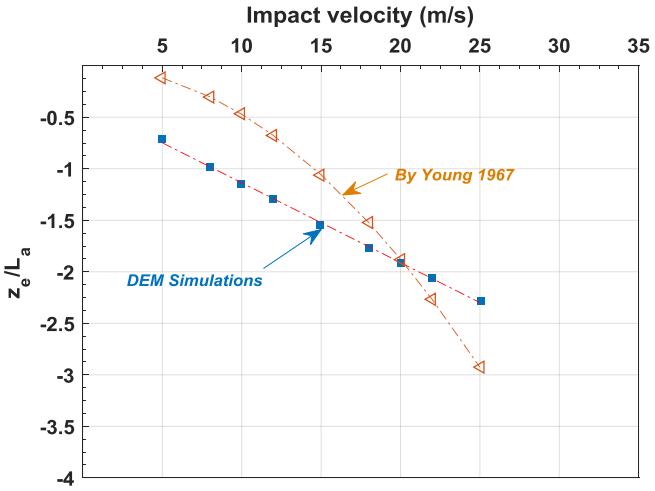

Figure 5. Comparison between DEM simulation and empirical equation developed by Young (1967).

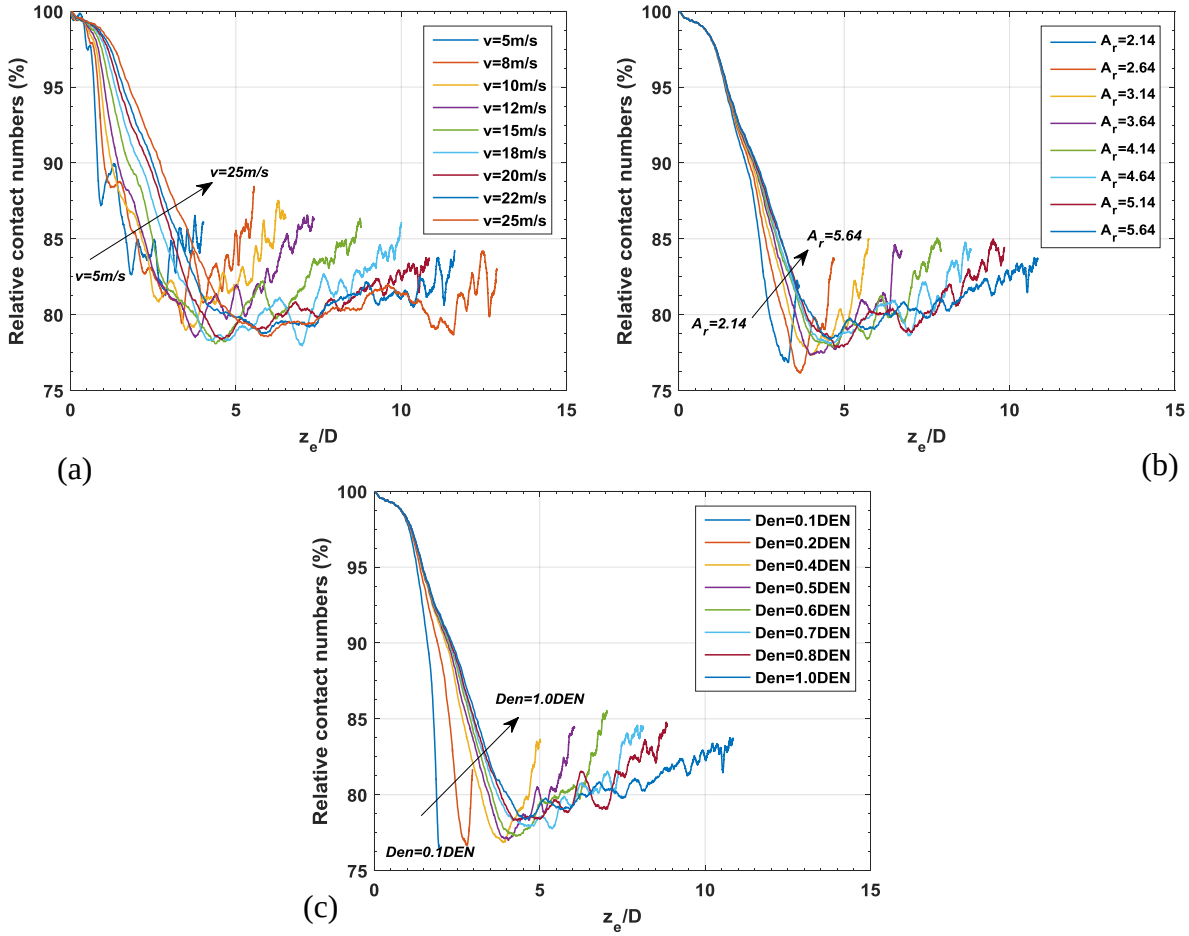

Figure 6. Contact numbers along with normalized penetration

CONCLUSIONS

DEM simulations were performed to investigate the influences of anchor penetration velocity, anchor shape, and anchor weight on penetration behavior. Anchor velocity profiles for different impact velocities were generated and maximum penetration depths under three different conditions are presented. The primary findings from this preliminary research are as follows:

1.) Under the same anchor weight and anchor shapes, the higher the anchor impact velocity, the higher the maximum penetration depth. The maximum penetration depth is around twice the anchor length.
2.) Maximum relative penetration depth increases linearly with the increase of impact velocity and anchor weight. The anchor aspect ratio has less significance on the penetration depth than impact velocity and anchor weight.
3.) DEM simulation results are aggressive and conservative at low and high impact velocities compared to empirical predictions.
4.) The penetration disturbs the particles at the soil surface and around the anchor tip. Particle contact loss is generally no more than 23%. The residual losses are around 15% compared to initial.

ACKNOWLEDGMENTS

This material is based upon work supported by the Department of Energy under Award Number DE-FG36-08GO18179. This report was prepared as an account of work sponsored by an agency of the United States Government. Neither the United States Government nor any agency thereof, nor any of their employees, makes any warranty, expressed or implied, or assumes any legal liability or responsibility for the accuracy, completeness, or usefulness of any information, apparatus, product, or process disclosed, or represents that is use would not infringe privately owned rights. The views and opinions of the authors expressed herein do not necessarily state or reflect those of the United States Government or any agency thereof.

REFERENCES

Audibert, J.M., Movant, M.N., Jeong-Yun, W., and Gilbert, R.B. (2006). Torpedo piles: laboratory and field research. In *The Sixteenth International Offshore and Polar Engineering Conference*. International Society of Offshore and Polar Engineers.

Boguslavskii, Y., Drabkin, S., and Salman, A. (1996). Analysis of vertical projectile penetration in granular soils. *Journal of Physics D: Applied Physics*, 29(3), 905.

Ciantia, M. O., Arroyo, M., Butlanska, J., & Gens, A. (2016). DEM modelling of cone penetration tests in a double-porosity crushable granular material. *Computers and Geotechnics*, 73, 109-127.

Ehlers, C.J., Young, A.G., and Chen, J.H. (2004). Technology assessment of deepwater anchors. In *Offshore technology conference*. Offshore Technology Conference.

Evans, T.M., and J.D. Frost. (2010). "Multiscale Investigation of Shear Bands in Sand: Physical and Numerical Experiments," *International Journal for Numerical and Analytical Methods in Geomechanics*, 34(15), pp. 1634-1650.

Evans, T.M. and J.G. Kress. (2011). "Discrete simulations of particulate-structure interactions," ASCE GeoFrontiers 2011, *Geotechnical Special Publication No. 211: Advances in Geotechnical Engineering*, Dallas, TX, pp. 4252-4262.

Fragaszy, R.J., and Taylor, T.A. (1989). Centrifuge Modeling of Projectile Penetration in Granular Soils (NO. ESL-TR-88-76). Dept. of Civil and Environmental Engineering, Washington State University, Pullman.

Freeman, T. J., Murray, C. N., and Schuttenhelm, R. T. E. (1988). The Tyro 86 penetrator experiments at Great Meteor East. In *Oceanology'88: Proceedings of an international conference*. Society of Underwater Technology.

Frost, J.D., G.L. Hebeler, T.M. Evans, and J.T. DeJong. (2004). Interface Behavior of Granular Soils. *Proceedings of the 9th ASCE Aerospace Division International Conference on Engineering, Construction, and Operations in Challenging Environments*, Houston, TX, USA, pp. 65-72.

Frost, J.D., T.M. Evans, Y. Lu, and X. Zhao. (2012). Selected observations from 3-D experimental and numerical studies of shear banding in biaxial shear tests. ASCE Geo-Congress 2012, *Geotechnical Special Publication No. 225: State of the Art and Practice in Geotechnical Engineering*, Oakland, CA, pp. 1116-1125.

Hall, W.S., and Oliveto, G. (2003). *Boundary Element Methods for Soil-Structure Interaction*. Springer Science and Business Media.

Hossain, M. S., O'Loughlin, C. D., and Kim, Y. (2015). Dynamic installation and monotonic pullout of a torpedo anchor in calcareous silt. *Géotechnique*, 65(2), 77-90.

Jacobson, D.E., J.R. Valdes, and T.M. Evans. (2007). A numerical view into direct shear specimen size effects. ASTM *Geotechnical Testing Journal*, 30(6), pp. 512-516.

Kausel, E. (2010). Early history of soil–structure interaction. *Soil Dynamics and Earthquake Engineering*, 30(9), 822–832.

Kress, J.G. and T.M. Evans. (2010). Analysis of pile behavior in granular soils using DEM. *Proceedings of the 35th Annual Deep Foundations Institute Annual Conference*, Hollywood, CA, October 12-15.

Lieng, J. T., Hove, F., and Tjelta, T. I. (1999). Deep Penetrating Anchor: Subseabed deepwater anchor concept for floaters and other installations. In *The Ninth International Offshore and Polar Engineering Conference*. International Society of Offshore and Polar Engineers.

Lieng, J.T., Kavli, A., and Tjelta, T.I. (2000). Deep penetrating anchor: further development, optimization and capacity clarification. Presented at the *10th International Offshore and Polar Engineering Conference*, International Society of Offshore and Polar Engineers.

Medeiros Jr, C. J. (2002). Low cost anchor system for flexible risers in deep waters. In *Offshore Technology Conference*. Offshore Technology Conference.

O'Beirne, C., O'Loughlin, C.D., Wang, D., and Gaudin, C. (2015). Capacity of dynamically installed anchors as assessed through field testing and three-dimensional large-deformation finite element analyses. *Canadian Geotechnical Journal*, 52(5), 548–562.

O'Loughlin, C., Richardson, M.D., Randolph, M.F., and Gaudin, C. (2013). Penetration of dynamically installed anchors in clay. *Géotechnique*, 63(11), 909–919.

Pyrz, A.P. (1969). Gravity Effects on Low Velocity Penetration of a Projectile into a Cohesionless Medium (No. GSF/MC/69-6). MS Thesis, Air Force Institute of Technology, Wright-Patterson AFB, OH.

Puthoff, R.L. (1971). High Speed Impact Tests of a Model Nuclear Reactor Containment System. NASA TM X-67856.

Raie, M.S., and Tassoulas, J.L. (2009). Installation of torpedo anchors: numerical modeling. *Journal of Geotechnical and Geoenvironmental Engineering*, 135(12), 1805-1813.

Shahin, M. A., and Jaksa, M. B. (2006). Pullout capacity of small ground anchors by direct cone penetration test methods and neural networks. *Canadian Geotechnical Journal*, 43(6), 626-637.

Taylor, T., Fragaszy, R.J. and Ho, C.L. (1991). Projectile penetration in granular soils. *Journal of Geotechnical Engineering*, 117(4), 658-672.

True, D.G. (1975). Penetration of projectiles into seafloor soils (No. CEL-TR-822). Civil Engineering LAB (NAVY) Port Hueneme CA.

Van Vooren, A., Borg, J., Sandusky, H., and Felts, J. (2013). Sand Penetration: A Near Nose Investigation of a Sand Penetration Event. *Procedia Engineering*, 58, 601-607.

Wang, W.L. (1969). Experimental study of projectile penetration in Ottawa sand at low velocities. *Journal of Spacecraft and Rockets*, 6(4), 497-498.

Wang, W.L. (1971). Low velocity projectile penetration. *Journal of the Soil Mechanics and Foundations Division*, 97(12), 1635-1655.

Young, C.W. (1967). The Development of Empirical Equations for Predicting Depth of an Earth-Penetrating Projectile. Rep. SC-DR-67-60, Sandia. Laboratories, May.

Zhang, N. and T.M. Evans. (2016). "Towards Anchoring of Marine Hydrokinetic Energy Devices: Three Dimensional Discrete Element Method Simulations of Interface Shear." To appear in *GeoChicago Geotechnical Special Publication*.

Zhao, X. and T.M. Evans. (2009). "Discrete Simulations of Laboratory Loading Conditions," *International Journal of Geomechanics*, 9(4), pp. 169-178.

Zhao, X. and T.M. Evans. (2011). "Numerical Analysis of Critical State Behaviors of Granular Soils Under Different Loading Conditions," *Granular Matter*, 13(6), pp. 751-764.